Development 135, 23-32 (2008) doi:10.1242/dev.007120

# Differential transmission of MEKK1 morphogenetic signals by JNK1 and JNK2

**Atsushi Takatori[1], Esmond Geh[1], Liang Chen[1], Lin Zhang[1,2], Jarek Meller[1] and Ying Xia[1,*]**

JNK1 and JNK2 are two ubiquitously expressed isoforms that exert redundant roles in many physiological processes, but the extent of their relative contributions to these processes has not been well characterized. We show that both JNK isoforms transmit MEK kinase 1 (MEKK1)-mediated morphogenetic signals during mouse embryonic eyelid closure. However, JNK1 and JNK2 are not synonymous, because MEKK1 is haploinsufficient for normal eyelid closure in *Jnk1*-null mice, but is haplosufficient in *Jnk2*-null mice. In the *Mekk1* heterozygous background, a more efficient phosphorylation of JNK1 than JNK2 leads to differential downstream reactions, such as c-Jun phosphorylation and PAI1 expression in the developing eyelid epithelium. Differences in efficiency of phosphorylation are attributed to JNK1 Gly177 and Ser179 – residues that are absent in JNK2 – which promote a less ordered structural conformation. This leads to more favorable JNK phosphorylation by activin B morphogenetic signals mediated by the MEKK1-MKK4 pathway. Interestingly, *Mekk1-Jnk1-Jnk2* triple hemizygotes display a partial eye-open phenotype at birth, suggesting that all three genes dose-dependently contribute to morphogenetic eyelid closure. We propose that a MEKK1-JNK1/2 axis governs the JNK activation levels to control downstream transcriptional events and eyelid morphogenesis and that reduction of upstream MEKK1 signals uncovers analogous but differential roles of JNK1 and JNK2 in a biological process.

**KEY WORDS: c-Jun, Epithelial morphogenesis, JNK isoforms, MEKK1/PAI1**

## INTRODUCTION

Jun N-terminal kinases (JNKs) are members of the mitogen-activated protein kinase (MAPK) family, playing a pivotal role in the transmission of extracellular signals through the cytosol to the nucleus. JNK activation is mediated by a cascade involving a MAPK kinase kinase (MAP3K)-MAPK kinase (MAP2K) signaling module, where extracellular signals first activate the MAP3K leading to the activation of MAP2K, which in turns activates JNK (Davis, 2000). At least 14 MAP3Ks, such as MEKK1-MEKK4, ASK1, MLKs and TAK1, are involved in mediating diverse upstream signals to the JNK pathway (Schlesinger et al., 1998), but only two MAP2K isoforms, MKK4 and MKK7, are directly responsible for JNK phosphorylation at threonine and tyrosine residues. Phosphorylation results in JNK activation and translocation to the nucleus, where JNK phosphorylates transcription factors. Following this paradigm, JNK plays a crucial role in converting transient biochemical signals to permanent changes of gene expression thereby participating in numerous physiological and pathological processes, such as immunity, neuronal development and cancer (Chang et al., 2003; Chen et al., 2001; Dong et al., 1998; Han et al., 2002; Kuan et al., 1999; Sabapathy et al., 2001).

Mammals have three distinct *Jnk* genes, two of which encode proteins JNK1 and JNK2 that are ubiquitously expressed, whereas expression of the JNK3 is restricted to the brain (Kyriakis et al., 1995). None of the mammalian JNKs are essential by themselves for fetal development, because all individual *Jnk* gene knockout mice survive embryonic development and are born with no overt phenotype (Dong et al., 1998; Sabapathy et al., 2001). Compound knockout $Jnk1^{-/-}Jnk2^{-/-}$ fetuses die on the twelfth day of gestation because of a disturbed apoptotic program in the brain, whereas $Jnk1^{-/-}Jnk3^{-/-}$ and $Jnk2^{-/-}Jnk3^{-/-}$ double knockouts have a normal appearance (Kuan et al., 1999). These observations suggest that the JNKs, especially the coexpressed JNK1 and JNK2, are functionally redundant in development. JNK1 and JNK2 share 83% amino acid sequence identity (Derijard et al., 1994) and early biochemical studies and recent chemical genetic data have indeed pointed at a similar substrate specificity and biological function for the two JNK isoforms (Derijard et al., 1994; Ventura et al., 2006).

Detailed genetic analyses indicate that JNK1 and JNK2 are not entirely equivalent, because many $Jnk1^{-/-}Jnk2^{+/-}$ mice suffer defective closure of optical fissure and eyelid and die shortly after birth, in clear contrast to the $Jnk1^{+/-}Jnk2^{-/-}$ mice, which develop normally (Weston et al., 2003). The functional differences between JNK1 and JNK2 have been mainly attributed to their substrate preferences and localization selectivity (Bocco et al., 1996; Eminel et al., 2004; Gao et al., 2004; Gdalyahu et al., 2004). Nevertheless, it has recently been shown that TNFα specifically activates JNK1 and not JNK2, suggesting that the JNK isoforms may be different in the way they connect to upstream pathways (Liu et al., 2004).

One ancestral function of JNK is found in the fruit fly, where it controls epithelial morphogenesis. Mutation of the *Drosophila Jnk* leads to defective dorsal epithelial cell migration and closure, giving rise to a lethal dorsal open phenotype (Noselli and Agnes, 1999; Sluss et al., 1996). We have previously shown that the mammalian MAP3K MEKK1 exhibits a distinct physiological function in epithelial morphogenesis. MEKK1-deficient mice are born with a relatively normal appearance but show an eye-open-at-birth (EOB) phenotype, owing to defective embryonic eyelid closure (Zhang et al., 2003). Eyelid closure is a process requiring eyelid epithelium extension and fusion, which takes place at embryonic day (E)15-E16. Interestingly, the morphogenetic features of eyelid closure are extremely similar to the corresponding dorsal closure of the fruit fly regulated by DJNK (Xia and Karin, 2004). Although MEKK1

[1]Department of Environmental Health and Center of Environmental Genetics, University of Cincinnati Medical Center, 123 E. Shields Street, Cincinnati, OH 45267-0056, USA. [2]Department of Central Lab, Southern Medical University, Tonghe, Guangzhou, People's Republic of China.

*Author for correspondence (e-mail: xiay@email.uc.edu)

**Accepted 1 October 2007**

ablation is associated with decreased JNK activation, clear genetic evidence for a role of JNK in eyelid closure is lacking (Zhang et al., 2003).

In this report, we provide genetic and biochemical data for the distinct roles of JNK1 and JNK2 in transmitting MEKK1 signals. Specifically, the MEKK1-mediated eyelid closure signals lead to differential phosphorylation of the two JNK isoforms, which as a consequence, make unique contributions to the downstream transcriptional events, leading to gene expression, epithelial cell migration and eyelid closure. Differences at amino acids 177 and 179 in the variable region of JNK1 and JNK2 determine their structural conformation and effectiveness of being phosphorylated.

## MATERIALS AND METHODS

### Mice, reagents and antibodies

The colonies of *Mekk1*$^{\Delta KD/\Delta KD}$ (*M1*$^{\Delta KD/\Delta KD}$), *Jnk1* knockout (*J1*$^{-/-}$) and *Jnk2* knockout (*J2*$^{-/-}$), mice have been described (Sabapathy et al., 1999; Sabapathy et al., 2001; Zhang et al., 2003) and wild-type C57/BL6 mice were purchased from Jackson Laboratory (Bar Harbor, ME). Intercrosses were carried out to generate compound mutant mice, including the *Mekk1*$^{+/\Delta KD}$*Jnk1*$^{+/-}$ (*M1*$^{+/\Delta KD}$*J1*$^{+/-}$), *Mekk1*$^{+/\Delta KD}$*Jnk1*$^{-/-}$ (*M1*$^{+/\Delta KD}$*J1*$^{-/-}$), *Mekk1*$^{+/\Delta KD}$*Jnk2*$^{-/-}$ (*M1*$^{+/\Delta KD}$*J2*$^{-/-}$) and *Mekk1*$^{+/-\Delta KD}$*Jnk1*$^{+/-}$*Jnk2*$^{+/-}$ (*M1*$^{+/\Delta KD}$*J1*$^{+/-}$*J2*$^{+/-}$) mice. All mice were maintained at the Experimental Animal Laboratory at the University of Cincinnati and the procedures conducted with these animals have been approved by the University of Cincinnati Animal Care and Use Committee.

The keratinocyte growth media (KGM) were from Cascade Biologicals and all other cell culture reagents were from Invitrogen. The growth factors, TGFα and TGFβ1 were from PeproTech, and activin B was from R&D Systems. SP600125 (SP), a JNK inhibitor, was from Calbiochem. The 4′-6-diamidine-2-phenylindole (DAPI), 5-bromo-2-deoxyuridine (BrdU) and the anti-hemagglutin (HA) agarose beads were from Sigma. Phospho-JNK antibody was from Promega; antibodies for phospho-c-Jun, phospho-ERK, phospho-EGFR, phospho-Smad2, phospho-MKK4, phospho-MKK7, MKK4 and MKK7 were from Cell Signaling; antibodies for JNK, c-Jun, JunD and phospho-Elk were from Santa Cruz Biotechnology, anti-PAI1 was from American Diagnostica and the anti-MEKK1 antibody was described previously (Xia et al., 1998). The active MKK4, JNK1 and JNK2, and c-Jun proteins were from Upstate Biotechnology.

Adenoviruses containing cDNA for an N-terminal hemagglutin (HA)-tagged human MEKK1 [MEKK1(WT)] or for HA- MEKK1(KM), a ATP-binding site mutant, were described elsewhere (Deng et al., 2006). The plasmids for Exp-MEKK1, HA-JNK1 and HA-JNK2 were described previously (Xia et al., 1998) and the plasmids for HA-JNK1(CTN) and HA-JNK2 (GTS) containing site-specific mutations at amino acids 177 and 179 sites were generated using a QuikChange site-directed mutagenesis kit (Stratagene).

### Cell culture

Mouse primary epidermal keratinocytes were prepared from newborn pups, as described (Zhang et al., 2003). Primary keratinocytes derived from each genotype were grown in KGM with supplementation of growth factors. The ES cells of wild type and *Mkk4*$^{-/-}$ were kindly provided by Dr Nishina and were maintained under conditions as described (Nishina et al., 1999). Mouse embryonic fibroblasts (MEFs) were prepared from E13.5 wild-type or mutant fetuses as described (Giroux et al., 1999) and HEK293 cells were from ATCC; both cells were cultured in DMEM supplemented with 10% fetal bovine serum.

### In vitro wound healing assay

Confluent monolayers of mouse primary epidermal keratinocytes were maintained in serum-free medium for 24 hours and pre-treated with or without 5 μM SP for 0.5 hour. A scratch wound was created with a micropipette tip and the cells cultured for 48 hours in the presence or absence of various growth factors, including TGFα (10 ng/ml), TGFβ1 (10 ng/ml) or activin B (5 ng/ml). In some experiments, SP 600125 (5 μM) was present in the medium. The wounds were photographed at 0 and 48 hours after wounding and the wound areas were measured in Photoshop. The wound-healing rate was calculated as the percentage of the remaining (at 48 hours) versus the original (at 0 hours) wound areas.

### Histology, immunohistochemistry and X-Gal staining

BrdU was injected intraperitoneally into pregnant dams at a dose of 100 mg/kg body weight 2 hours before autopsy. The E15.5-E19.5 fetuses and adult eye tissues were fixed in 4% paraformaldehyde, dehydrated with a graded ethanol series and embedded in paraffin. Sections (5 μm) were deparaffinized by immersing in xylene and rehydration, followed by staining with hematoxylin and eosin (H&E) according to standard procedures.

Sections were subjected to immunohistochemistry as described (Deng et al., 2006) using anti-phospho-JNK (1:1000), phospho-c-Jun (1:2000), phospho-MKK4 (1:100), phospho-MKK7 (1:100), JNK (1:100), phospho-Smad2 (1:200), phospho-EGFR (1:25), c-Jun (1:100), Jun D (1:100), C/EBPα (1:100), phospho-Elk (1:100), PAI1 (1:500), Keratin 6 (1:500), Keratin 10 (1:500) and BrdU (1:1000) antibodies. Whole-mount X-Gal staining of *J1*$^{-/-}$ and *J2*$^{-/-}$ fetuses was performed as described previously (Zhang et al., 2003).

### Cell treatment, transfection and adenoviral infection

Monolayers of epidermal keratinocytes, MEFs and ES cells at 80% confluency were treated with growth factors for the indicated times. Cell lysates were subjected to western blotting as described previously (Zhang et al., 2003). Transfection of HEK293 cells with plasmid DNA was done using lipofectamine plus (Invitrogen) as described (Xia et al., 1998). Infection by adenoviruses containing MEKK1 (WT) and MEKK1(KM) of the ES and MEFs was done as described (Deng et al., 2006). In brief, 10 pfu viral particles/cell were added to 80% confluent cells in culture. Following incubation for 1 hour, the virus was removed and the cells allowed to grow for 48 hours before harvesting.

### Immunoprecipitation, GST-c-Jun pull-down and western blot analyses

Cell lysates were prepared in lysis buffer (50 mM Tris-HCl, pH 7.2, 2 mM EDTA, 150 mM NaCl, 1% NP-40) followed by repeated freeze and thaw cycles. Cell lysates (200-500 μg) were incubated with appropriate antibodies for 1 hour at 4°C, followed by incubation with protein-A-agarose at 4°C overnight. In some experiments, the lysates were incubated with anti-HA beads (Sigma) at 4°C for 4-16 hours; in other experiments, lysates were incubated with GST-c-Jun agarose beads at 4°C for 4 hours. After extensive washing of the beads with lysis buffer, the immunoprecipitates or pull-down proteins were washed twice with kinase buffer (25 mM Tris-HCl pH 7.5, 5 mM $MgCl_2$, 1 mM EGTA, 2 mM dithiothreitol, 0.5 mM sodium vanadate and 25 mM β-glycerophosphate). The beads were either used for in vitro kinase assay or western blot analyses. For western blot analyses, the immunoprecipitates, pull-down proteins or 50-100 μg of total cell lysates were resolved on SDS-PAGE followed by western blot detection using appropriate antibodies.

### In vitro kinase assay

Immunoprecipitated or commercially purchased activated MKK4, JNK1 and JNK2 proteins were subjected to in vitro kinase assay using HA-JNK, GST-c-Jun (1-79) or c-Jun protein (Upstate Biotechnology) as a substrate. The kinase reaction was carried out in the presence of 0.2 μM ATP, 2.5 μCi [$\gamma$-$^{32}$P]ATP and 1× kinase buffer and the mixture was incubated at 30°C for 30 minutes. Following SDS-PAGE, the proteins were transferred to nitrocellulose membranes. The membranes were then exposed to X-ray film and subjected to western blot analysis.

### Computational analysis

The SABLE program (http://sable.cchmc.org) was used to analyze the differences in propensities for secondary structures between JNK isoforms and also between the phosphorylated and unphosphorylated peptides. Such analysis could indicate regions that may undergo a conformational transition and thus change the affinity for binding other proteins. Unlike other state-of-the-art methods, SABLE uses propensities and characteristics of individual amino acid residues, in addition to evolutionary profiles that

remain essentially unchanged for close homologs, to make predictions, and thus enables the analysis of putative effects of a limited number of point mutations (Adamczak et al., 2004).

## RESULTS

### MEKK1 is a rate-limiting factor for activation of the MKK4-JNK pathway

We have shown that MEKK1 ablation in mice causes defective eyelid closure during embryonic development and that the *Mekk1*$^{\Delta KD/\Delta KD}$ mice exhibit an EOB phenotype (Zhang et al., 2003). To search for the downstream effectors of MEKK1 during mouse embryonic eyelid development, we examined the E15.5 wild-type, *Mekk1*$^{+/\Delta KD}$ and *Mekk1*$^{\Delta KD/\Delta KD}$ fetuses for phosphorylation of MKK4 and MKK7, two MAP2Ks directly upstream of JNK. In wild-type fetuses, there was strong MKK4 phosphorylation in the developing eyelid epithelium, but only weak MKK7 phosphorylation was detected (Fig. 1A). Both phospho-MKK4 and phospho-MKK7 were considerably decreased in the *Mekk1*$^{+/\Delta KD}$ and almost completely diminished in the *Mekk1*$^{\Delta KD/\Delta KD}$ fetuses.

Activin B is a member of the TGFβ family and is abundantly expressed in the developing eyelid epithelium; importantly activin B (gene symbol *Inhbb* – Mouse Genome Informatics) knockout mice also display an EOB phenotype (Vassalli et al., 1994). We have previously shown that the activin B signals in eyelid closure are transmitted by MEKK1 (Zhang et al., 2003; Zhang et al., 2005). To characterize the involvement of MKK4 and MKK7 in the activin B and MEKK1 signaling, we examined their phosphorylation in mouse embryonic stem (ES) cells treated by activin B and infected by adenoviruses mediating MEKK1 overexpression. Although activin B and MEKK1 both caused a marked induction of MKK4 phosphorylation, they stimulated only a marginal MKK7 phosphorylation (Fig. 1B). Collectively, these data suggest that MEKK1 predominantly activates MKK4 over MKK7 in vivo and in vitro. Moreover, MKK4 was essential for transmission of the MEKK1 signals to activate JNK, because MEKK1-induced JNK phosphorylation took place in wild-type ES cells, but was completely abolished in *Mkk4*$^{-/-}$ cells (Fig. 1C).

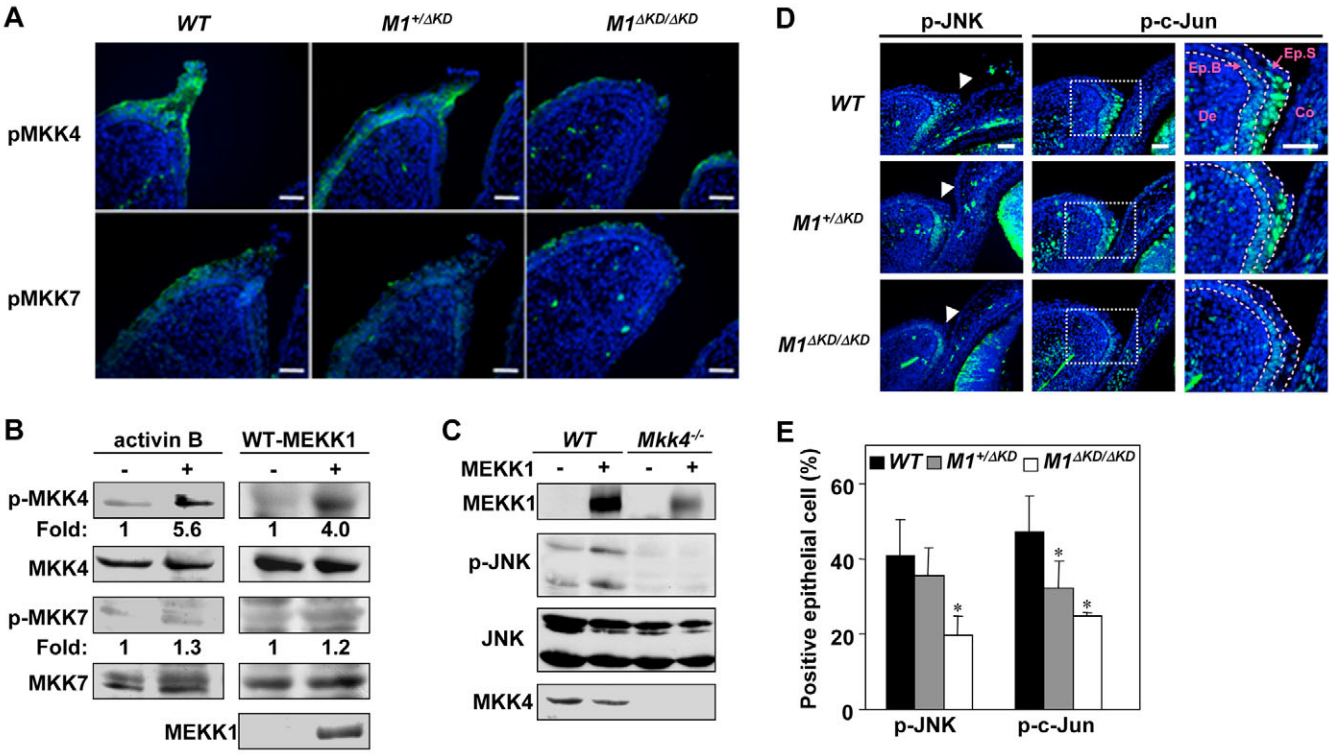


**Fig. 1. The MEKK1-MKK4 pathway leads to JNK and c-Jun phosphorylation in the developing eyelid epithelium.** (**A**) Immunofluorescence staining of wild-type (*WT*), *Mekk1*$^{+/\Delta KD}$ (*M1*$^{+/\Delta KD}$) and *Mekk1*$^{\Delta KD/\Delta KD}$ (*M1*$^{\Delta KD/\Delta KD}$) fetuses at embryonic day 15.5 (E15.5) for p-MKK4 (top panels) and p-MKK7 (bottom panels) (green). Nuclei are stained with DAPI (blue). Scale bars: 50 μm. The images are representative of at least three fetuses of each genotype examined. (**B**) Mouse embryonic stem (ES) cells were either left untreated or treated with activin B (5 ng/ml) for 10 minutes or infected with adenovirus for WT-MEKK1 for 24 hours, as labeled. The cell lysates were subjected to western blot analyses using antibodies for phosphorylated and total MKK4 and MKK7, and MEKK1, as indicated. The results were quantified by chemiluminescence imaging and the fold induction of p-MKK4 and p-MKK7 by activin B and MEKK1 over the control was calculated. (**C**) Wild-type and *Mkk4*$^{-/-}$ ES cells were infected with either control or WT-MEKK1 adenoviruses. At 24 hours post infection, cell lysates were examined by western blotting for phosphorylated and total JNK, MEKK1 and MKK4. (**D**) Immunofluorescence staining of wild- type (*WT*), *Mekk1*$^{+/\Delta KD}$ (*M1*$^{+/\Delta KD}$) and *Mekk1*$^{\Delta KD/\Delta KD}$ (*M1*$^{\Delta KD/\Delta KD}$) fetuses at embryonic day 15.5 (E15.5) detected phospho-JNK (p-JNK) (left panels) and phospho-c-Jun (p-c-Jun) (middle panels) (green) in the developing eyelid epithelium (arrowheads). Nuclei were stained with DAPI (blue). White rectangular areas of p-c-Jun staining (middle panels) are also shown at higher magnification (right panels). Dotted lines mark dermis (De), basal epithelial layer (Ep. B), suprabasal epithelial layer (Ep. S) and cornea (Co). Scale bars, 50 μm. At least four fetuses (8 eyes) of each genotype were examined. (**E**) The fraction of phosphorylation-positive cells over total cell count in suprabasal epithelial layer was calculated and statistically significant differences ($P$<0.05) from wild-type fetuses are denoted with an asterisk.

To investigate whether JNK was downstream of the MEKK1-MKK4 pathway during mouse embryonic eyelid closure, we examined E15.5 wild type, *Mekk1*$^{+/\Delta KD}$ and *Mekk1*$^{\Delta KD/\Delta KD}$ fetuses for phosphorylation of JNK. In wild-type fetuses, JNK was highly phosphorylated in the suprabasal layers of the developing eyelid epithelium, which harbor the MEKK1 expressing cells (Zhang et al., 2003), and less phosphorylated in the basal layers (Fig. 1D). In *Mekk1*$^{\Delta KD/\Delta KD}$ fetuses, phosphorylation of JNK was markedly reduced. A similar MEKK1-dependent phosphorylation pattern was observed for c-Jun, one of the well-known JNK substrates and a component of the AP-1 transcription complex. Interestingly, *Mekk1* heterozygous (*Mekk1*$^{+/\Delta KD}$) mice showed consistently reduced levels of MKK4, JNK and c-Jun phosphorylation, even though they had normal eyelid closure like their wild-type littermates (Fig. 1A,D). The number of phosphorylation positive cells detected in the *Mekk1*$^{+/\Delta KD}$ fetuses was lower than in wild type, but greater than in

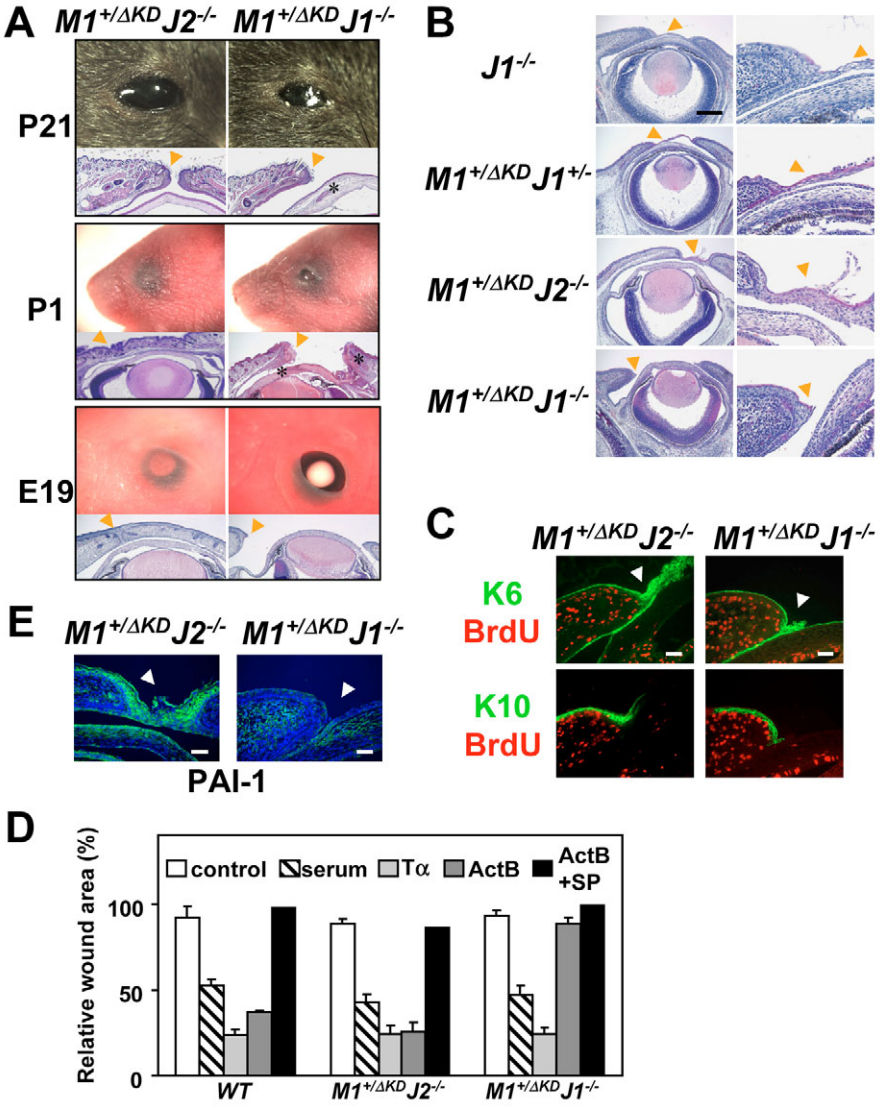


**Fig. 2. Defective embryonic eyelid closure of the *Mekk1*$^{+/\Delta KD}$*Jnk1*$^{-/-}$ mice and impaired migration of the *Mekk1*$^{+/\Delta KD}$*Jnk1*$^{-/-}$ keratinocytes.** (**A**) Photographs and histological analyses (H&E) of the eyes in *Mekk1* heterozygous *Jnk1*-null (*M1*$^{+/\Delta KD}$*J1*$^{-/-}$) and *Mekk1* heterozygous *Jnk2*-null (*M1*$^{+/\Delta KD}$*J2*$^{-/-}$) mice at E19, postnatal day (P)1 and P21. The *M1*$^{+/\Delta KD}$*J1*$^{-/-}$ mice have impaired developmental eyelid closure and an EOB phenotype. H&E staining of the eye tissue sections show developmental eyelid (arrowheads) and ocular tissue inflammation (asterisk). (**B**) H&E staining of the developing eye at E16. The *Jnk1*-null (*J1*$^{-/-}$), *M1*$^{+/\Delta KD}$*J1*$^{+/-}$ and *M1*$^{+/\Delta KD}$*J2*$^{-/-}$ fetuses had eyelid epithelium (arrowheads) covered ocular surface, whereas the *M1*$^{+/\Delta KD}$*J1*$^{-/-}$ fetus had opened eyelids and fully exposed ocular surface. Scale bar: 200 μm. (**C**) Immunofluorescence staining for BrdU (red) and keratins (green) of the developing eyes at E16. Similar levels of keratin 6 (K6) and keratin 10 (K10) expression and BrdU incorporation were detected in the developing eyelid epithelium of *M1*$^{+/\Delta KD}$*J1*$^{-/-}$ and *M1*$^{+/\Delta KD}$*J2*$^{-/-}$ fetuses. (**D**) An in vitro wound healing assay was performed on mouse primary epidermal keratinocytes isolated from wild-type, *M1*$^{+/\Delta KD}$*J1*$^{-/-}$ and *M1*$^{+/\Delta KD}$*J2*$^{-/-}$ mice, in the presence or absence of 10% fetal bovine serum (serum), individual growth factors, TGFα (Tα) and activin B (Act B), or the JNK inhibitor (SP), as indicated. Photographs were taken immediately and 48 hours after wounding. The remaining wound areas at 48 hours were compared with the original wound area. The results represent the mean ± s.d. of at least four independent experiments. (**E**) Immunofluorescence staining showed PAI1 expression (green) was abundant in developing eyelid epithelium of the *M1*$^{+/\Delta KD}$*J2*$^{-/-}$, but was almost undetectable in that of the *M1*$^{+/\Delta KD}$*J1*$^{+/-}$ fetuses. Nuclei were stained with DAPI (blue). Arrowheads indicate the developing eyelid tip. Scale bars: 50 μm.

MEKK1-null fetuses, suggesting that limiting the amount of MEKK1 may reduce the level of downstream JNK activation in the developing eyelid epithelium (Fig. 1E).

## Genetic evidence for the involvement of JNK in embryonic eyelid closure and epithelial cell migration

To test whether the JNK1 or JNK2 isoform alone was sufficient for eyelid development when MEKK1 was reduced, we generated *Jnk1*$^{-/-}$ and *Jnk2*$^{-/-}$ mice in the *Mekk1* heterozygous genetic background. At E19, *Mekk1*$^{+/\Delta KD}$*Jnk2*$^{-/-}$ mice showed normal eyelid development; however, the *Mekk1*$^{+/\Delta KD}$*Jnk1*$^{-/-}$ mice displayed EOB like *Mekk1*$^{\Delta KD/\Delta KD}$ mice (Zhang et al., 2003) (Fig. 2A). Histological analyses indicated that E16 *Mekk1*$^{+/\Delta KD}$*Jnk1*$^{-/-}$ fetuses lacked eyelid epithelial extension and fusion (Fig. 2B), which resulted in the defective eyelid closure observed at E19, and severe inflammation in eyelid and cornea at various postnatal developmental stages (Fig. 2A).

Eyelid epithelial cell proliferation and differentiation are required for embryonic eyelid closure. We found that proliferation and differentiation did not account for the striking differences in eyelid closure of *Mekk1*$^{+/\Delta KD}$*Jnk2*$^{-/-}$ and *Mekk1*$^{+/\Delta KD}$*Jnk1*$^{-/-}$ embryos, because fetuses of the two genotypes displayed similar levels of proliferating (BrdU-positive), basal (K6-positive) and suprabasal (K10-positive) epithelial cells in the developing eyelid (Fig. 2C).

The epithelial cell migration to the center of the eye is another crucial activity required for embryonic eyelid closure. To examine epithelial cell migration, we used an in vitro wound-healing assay using keratinocytes isolated from wild-type, *Mekk1*$^{+/\Delta KD}$*Jnk2*$^{-/-}$ and *Mekk1*$^{+/\Delta KD}$*Jnk1*$^{-/-}$ mice. When treated with serum or TGFα, all cells showed increased migration and significantly reduced wound area, suggesting that these cells contain all the essential components for migration and wound closure (Fig. 2D); when treated with activin B, only the wild-type and *Mekk1*$^{+/\Delta KD}$*Jnk2*$^{-/-}$ cells displayed increased migration, but the *Mekk1*$^{+/\Delta KD}$*Jnk1*$^{-/-}$ cells failed to do so. In agreement with previous findings that activin B stimulated migration through the MEKK1-JNK pathway (Zhang et al., 2003; Zhang et al., 2005), a JNK inhibitor completely abolished the induction of migration (Fig. 2D).

Induction of cell migration by activin B is mediated, at least partly, through activation of gene expression. We have previously identified plasminogen activator inhibitor 1 (*PAI1* also known as *Serpine1* – Mouse Genome Informatics) as a target gene of the activin-B-induced MEKK1 pathway, and more importantly, *PAI1* expression is essentially required for epithelial cell migration (Deng et al., 2006). We found that PAI1 was highly expressed in the eyelid epithelial cells of *Mekk1*$^{+/\Delta KD}$*Jnk2*$^{-/-}$, but was almost completely absent in *Mekk1*$^{+/\Delta KD}$*Jnk1*$^{-/-}$ fetuses (Fig. 3C). Hence, defective eyelid closure in the *Mekk1*$^{+/\Delta KD}$*Jnk1*$^{-/-}$ fetuses may be attributed at least in part to lacking PAI1 expression, and consequently, impaired eyelid epithelial cell migration.

## Reduced JNK activation in the *Mekk1*$^{+/\Delta KD}$*Jnk1*$^{-/-}$ developing eyelid epithelium and keratinocytes

Despite their striking differences in eyelid closure, the *Mekk1*$^{+/\Delta KD}$*Jnk1*$^{-/-}$ and *Mekk1*$^{+/\Delta KD}$*Jnk2*$^{-/-}$ fetuses had equal levels of JNK expression in the developing eyelid (Fig. 3A). Additionally, similar levels of β-galactosidase activity were detected in the E15 *Jnk1*$^{-/-}$ and *Jnk2*$^{-/-}$ fetuses, which carry a bacterial β-galactosidase gene driven by the target-gene promoter, indicating equal activation of *Jnk1* and *Jnk2* promoters (Sabapathy et al., 2001) (Fig. 3C). However, there was an obvious difference in JNK phosphorylation between *Mekk1*$^{+/\Delta KD}$*Jnk1*$^{-/-}$ and *Mekk1*$^{+/\Delta KD}$*Jnk2*$^{-/-}$ fetuses (Fig. 3A). In comparison to wild-type,

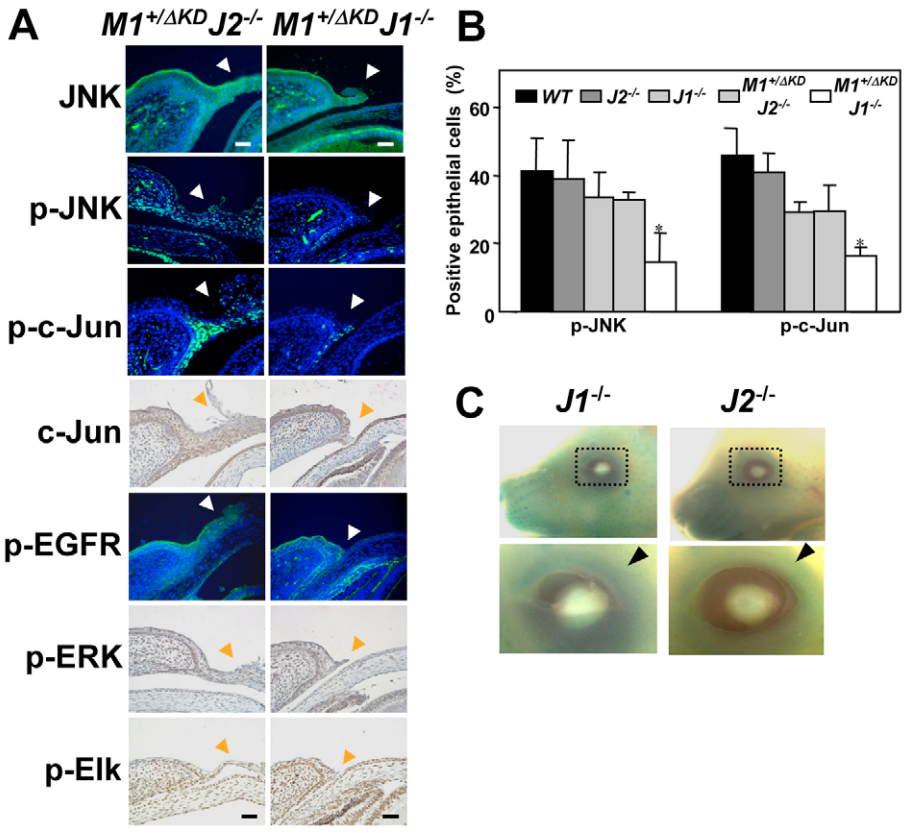


**Fig. 3. Reduction of JNK and c-Jun phosphorylation in *M1*$^{+/\Delta KD}$*J1*$^{-/-}$ eyelid epithelium.** (**A**) The *M1*$^{+/\Delta KD}$*J1*$^{-/-}$ and *M1*$^{+/\Delta KD}$*J2*$^{-/-}$ fetuses at E15.5 were examined by immunohistochemistry for the phospho- and total JNK and c-Jun, phospho-EGFR (p-EGFR), phospho-ERK (p-ERK) and phospho-Elk (p-Elk). Levels of only p-JNK and p-c-Jun were significantly reduced in the developing eyelid epithelium of the *M1*$^{+/\Delta KD}$*J1*$^{-/-}$ fetuses. Scale bars: 50 μm. (**B**) Quantitative summary of the percentage of p-JNK- and p-c-Jun-positive cells in suprabasal epithelial layers of the developing eyelids in various gene knockout fetuses. Data are mean ± s.d. of at least four fetuses of each genotype examined. Only the *M1*$^{+/\Delta KD}$*J1*$^{-/-}$ fetuses showed significant (**P*<0.01) reduction in p-JNK and p-c-Jun compared with wild-type fetuses. (**C**) E15.5 *Jnk1*-null (*J1*$^{-/-}$) and *Jnk2*-null (*J2*$^{-/-}$) fetuses were subjected to X-Gal staining to detect the target gene promoter-driven β-galactosidase expression. X-Gal-positive cells were detected in the entire embryonic body of E15.5 fetuses. Arrowheads indicate the developing eyelid tip.

*Jnk1*$^{-/-}$, *Jnk2*$^{-/-}$ and *Mekk1*$^{+/\Delta KD}$*Jnk2*$^{-/-}$ fetuses, the *Mekk1*$^{+/\Delta KD}$*Jnk1*$^{-/-}$ had significantly less JNK phosphorylation in the eyelid epithelium (Fig. 3A,B).

To search for additional molecular alterations in the *Mekk1*$^{+/\Delta KD}$*Jnk1*$^{-/-}$ fetuses, we examined the expression or phosphorylation of nuclear factors, including c-Jun, JunD, c-Fos, Elk-1, c/EBPα, c/EBPβ and Smad2 (Bogoyevitch and Kobe, 2006). Of these factors, only phospho-c-Jun was induced at lower levels in the eyelid epithelium of *Mekk1*$^{+/\Delta KD}$*Jnk1*$^{-/-}$ than in that of *Mekk1*$^{+/\Delta KD}$*Jnk2*$^{-/-}$ fetuses (Fig. 3A,B and see Fig. S1 in the supplementary material). The role of c-Jun in eyelid closure might be through the induction of heparin-binding EGF to activate the epidermal growth factor receptor (EGFR)-ERK pathway (Li et al., 2003); however, there was no difference in the phosphorylation of EGFR, ERK and Elk in developing eyelid epithelium of *Mekk1*$^{+/\Delta KD}$*Jnk1*$^{-/-}$ and *Mekk1*$^{+/\Delta KD}$*Jnk2*$^{-/-}$ fetuses, excluding differential EGFR pathway activation in these fetuses (Fig. 3A). Thus, the only molecular changes we have identified in the *Mekk1*$^{+/\Delta KD}$*Jnk1*$^{-/-}$ developing eyelid epithelium are insufficient phosphorylation of JNK2 and c-Jun.

We further examined JNK phosphorylation in *Mekk1*$^{+/\Delta KD}$*Jnk1*$^{-/-}$ and *Mekk1*$^{+/\Delta KD}$*Jnk2*$^{-/-}$ keratinocytes exposed to several morphogenetic factors, including TGFα, TGFβ1 and activin B. Cells from both genotypes had very similar levels of JNK and c-Jun expression; however, JNK1 phosphorylation was highly induced by TGFα, TGFβ1 and activin B in *Mekk1*$^{+/\Delta KD}$*Jnk2*$^{-/-}$ cells, whereas induction of JNK2 phosphorylation was much weaker in *Mekk1*$^{+/\Delta KD}$*Jnk1*$^{-/-}$ cells (Fig. 4A). The Smad and ERK phosphorylation was induced equally well in both cells.

In *Mekk1*$^{+/\Delta KD}$*Jnk1*$^{-/-}$ cells, induction of phospho-JNK2 was two to three times greater with TGFα and TGFβ1 than with activin B (Fig. 4A and see Fig. S2 in the supplementary material). More strikingly, c-Jun phosphorylation, which was quite strongly induced by TGFα and TGFβ1, was completely undetectable after activin B treatment. To address whether the amount of MEKK1 was particularly crucial for transmission of activin B signals to JNK, we compared JNK2 and c-Jun phosphorylation in *Mekk1*$^{+/\Delta KD}$*Jnk1*$^{-/-}$ and *Jnk1*$^{-/-}$ keratinocytes treated with activin B and its related family member, TGFβ1. Although TGFβ1 activated JNK2/c-Jun in both cell types equally well, activin B effectively activated JNK2/c-Jun only in *Jnk1*$^{-/-}$cells (Fig. 4B,C). In *Mekk1*$^{+/\Delta KD}$*Jnk1*$^{-/-}$ cells, activin B induced marginal JNK2 activation, but no c-Jun phosphorylation, similarly to that observed in the developing eyelid epithelium of the corresponding fetuses (Fig. 3A, Fig. 4B,C). These observations suggest that the activin B signal transmitted through MEKK1 leads to more efficient phosphorylation of JNK1 than of JNK2.

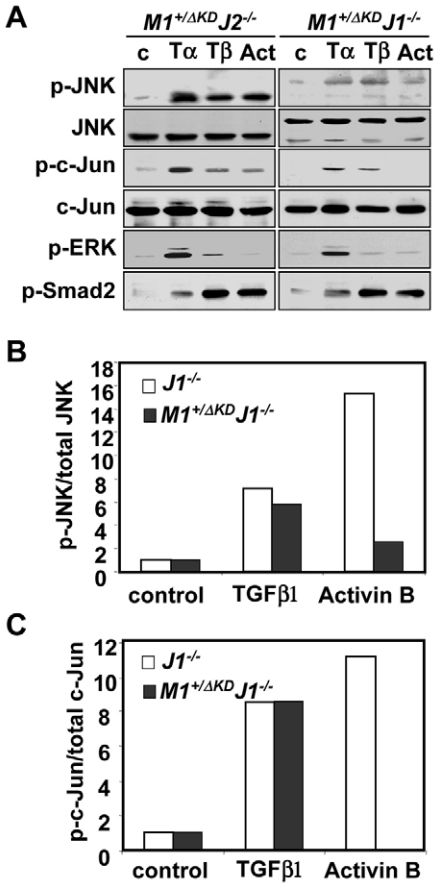


**Fig. 4. MEKK1 is required for efficient transmission of the activin B signals to JNK.** (**A**) *M1*$^{+/\Delta KD}$*J1*$^{-/-}$ and *M1*$^{+/\Delta KD}$*J2*$^{-/-}$ keratinocytes were either untreated (c) or treated with TGFα (Tα, 10 ng/ml), TGFβ1 (Tβ, 10 ng/ml) or activin B (Act, 5 ng/ml) for 10 minutes, and cell lysates were analyzed for phosphorylated and total JNK and c-Jun, phospho-ERK and phospho-Smad2 by western blotting. Similar results were obtained from at least two independent experiments. The relative ratio of (**B**) p-JNK/total JNK and (**C**) p-c-Jun/total c-Jun in the *Jnk1*-null (*J1*$^{-/-}$) and *M1*$^{+/\Delta KD}$*J1*$^{-/-}$ keratinocytes either untreated (control) or treated with TGFβ and activin B were quantified by chemiluminescence imaging analyses and represented graphically. The levels in untreated cells were used as a standard for quantification. Similar results were obtained from at least three independent experiments.

## The G177/S179 residues in the JNK1 activation loop determine the efficient phosphorylation of JNK1

Similarly to activin B, the MEKK1 itself also caused differential phosphorylation of JNK1 and JNK2, because when each JNK isoform was coexpressed with active MEKK1 in HEK293 cells, both were phosphorylated, but in relative terms, phospho-JNK1 was twice as high as phospho-JNK2 (Fig. 5A). One possible explanation why the MEKK1 signals lead to different JNK1 and JNK2 phosphorylation is that the JNK isoforms have different affinities of interaction with MEKK1 (Xu and Cobb, 1997). We tested this using adenovirus-mediated expression of HA-tagged MEKK1 in MEFs and examining its interaction with JNK1 and JNK2. Specifically, wild-type, *M1*$^{+/\Delta KD}$, *M1*$^{+/\Delta KD}$*J1*$^{-/-}$ and *M1*$^{+/\Delta KD}$*J2*$^{-/-}$ MEFs were either uninfected or infected with adenoviruses for HA-tagged kinase active MEKK1 [HA-MEKK1(WT)] or for kinase-inactive mutant MEKK1 [HA-MEKK1(KM)]. Cell lysates were subjected to immunoprecipitation using a mixture of anti-JNK1 and anti-JNK2 and the immunoprecipitates were analyzed by western blotting using anti-HA for MEKK1. We found that both endogenous JNK1 and JNK2 bound to and co-precipitated the HA-tagged MEKK1 in wild-type and *Mekk1*$^{+/\Delta KD}$ MEFs (Fig. 5B). Moreover, JNK2 in the *Mekk1*$^{+/\Delta KD}$*Jnk1*$^{-/-}$ and JNK1 in the *Mekk1*$^{+/\Delta KD}$*Jnk2*$^{-/-}$ MEFs exhibited the same binding efficiencies towards HA-MEKK1 (Fig. 5B,C). JNK1 and JNK2 interacted with both the wild-type active and the kinase-inactive MEKK1, suggesting that MEKK1 activity and JNK phosphorylation status had no impact on MEKK1-JNK1/2 complex formation.

Alternatively, the JNK isoforms may have structural differences that result in a differential rate of phosphorylation by MEKK1-mediated MKK4. To evaluate this possibility, we used the SABLE program (http://sable.cchmc.org) to assess the propensities for

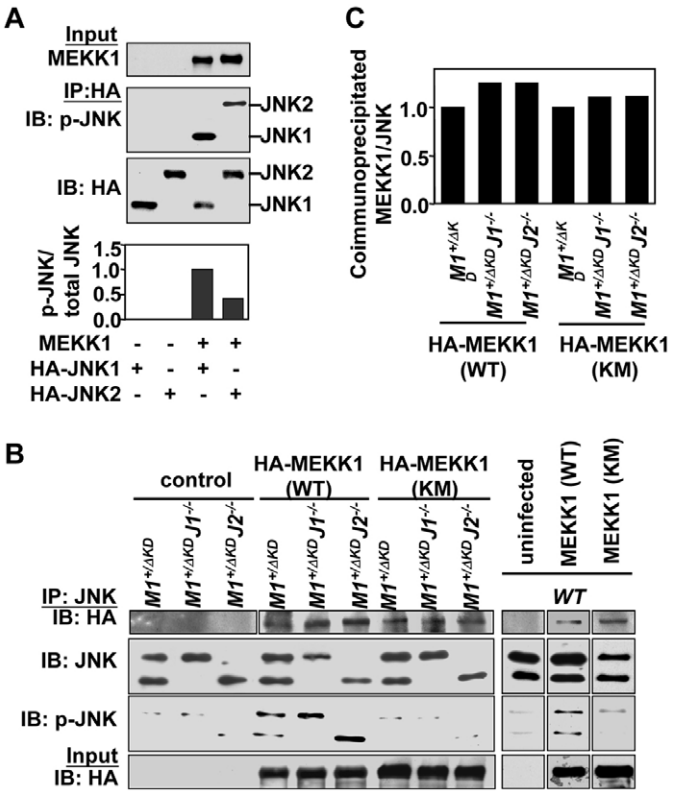


**Fig. 5. Differential activation of JNK1 and JNK2 by MEKK1.** (**A**) HEK293 cells were transiently co-transfected with plasmids for active MEKK1, HA-JNK1 and HA-JNK2 as indicated, and the JNKs were purified by immunoprecipitation using anti-HA. Cell lysates and immunoprecipitates were analysed by immunoblotting using anti-MEKK1, anti-p-JNK and anti-HA. The amount of phospho-JNK and total immunoprecipitated HA-JNK was quantified by chemiluminescence imaging and pJNK/JNK ratio is shown graphically. Similar results were obtained from at least three independent experiments. (**B**) Wild-type, $M1^{+/\Delta KD}$, $M1^{+/\Delta KD}J1^{-/-}$ and $M1^{+/\Delta KD}J2^{-/-}$ MEFs were either uninfected or infected with adenoviruses for HA-tagged kinase active MEKK1 [HA-MEKK1(WT)] or for the kinase-inactive mutant MEKK1 [HA-MEKK1(KM)]. Cell lysates were subjected to immunoprecipitation using a mixture of anti-JNK1 and anti-JNK2 and the immunoprecipitates were analyzed by western blotting using anti-HA, anti-JNK and anti-phospho-JNK antibodies. The experiments were repeated twice and the results were consistent. (**C**) The results in B were quantified by chemiluminescence imaging analyses and the co-immunoprecipitated MEKK1/JNK is represented graphically.

secondary structures of JNK1 and JNK2. Some subtle differences between JNK1 and JNK2 were indeed observed within the variable region (amino acids 173-190) of activation loop (Xie et al., 1998), where an additional β-strand was predicted in JNK2, but not in JNK1 (Fig. 6A and see Fig. S3A in the supplementary material). JNK1 and JNK2 are highly homologous in this region, except that JNK2 has Cys and Asn at position 177 and 179, respectively, whereas, JNK1 has Gly177 and Ser179 residues. It is possible that the Gly177/Ser179 residues of JNK1 are crucial for maintaining a less ordered conformation that has a lower propensity for β-sheet formation, and as a consequence, favors JNK phosphorylation.

To test this possibility, we generated JNK1(CTN) by replacing the JNK1 amino acids Gly177 and Ser179 with their JNK2 counterparts, Cys and Asn, respectively. Conversely, we generated JNK2(GTS) by replacing Cys177 and Asn179 of JNK2 with their Gly and Ser JNK1 counterparts. The hemagglutinin (HA)-tagged wild-type and mutant JNK1 and JNK2 were expressed in HEK293 cells and were isolated by immunoprecipitation. The immunoprecipitates were used for in vitro kinase assay in the presence of an active MKK4 and [$\gamma$-$^{32}$P]ATP (Fig. 6B). When equivalent amount of HA-proteins was assessed, the relative phosphorylation of wild-type JNK1 by MKK4 was 1.5 times greater than JNK1 (CTN). Conversely, the phosphorylation of the mutant JNK2 (GTS) was 1.6 times greater than its wild-type counterpart.

We further tested the JNK phosphorylation and catalytic activity in HEK293 cells. Expression of MEKK1 resulted in the phosphorylation of JNK1(CTN) that was reduced to half that of the parental JNK1, whereas the phosphorylation of JNK2(GTS) increased almost twofold relative to the parental JNK2 (Fig. 6C). To test whether the levels of JNK phosphorylation were relevant to JNK catalytic activity, we isolated JNK from transfected cells and subjected it to immune complex kinase assay to measure its ability to phosphorylate c-Jun. The JNK activity correlated with its phosphorylation status; thus, wild-type JNK1 and JNK2 (GTS) were stronger than JNK1(CTN) and wild-type JNK2 in their ability to phosphorylate c-Jun (Fig. 6D). Hence, the GTS sequence motif within the activation loop offers a higher phosphorylation efficiency and therefore functional activation of JNK1 over JNK2.

### *Mekk1*, *Jnk1* and *Jnk2* gene dosage sets the threshold for eyelid epithelial morphogenesis

The differential activation efficiencies may explain why JNK1 and JNK2 are not making equal contributions to eyelid development. $M1^{+/\Delta KD}J1^{-/-}$ mice have low JNK phosphorylation and EOB, whereas, the $M1^{+/\Delta KD}J2^{-/-}$ mice have high JNK phosphorylation and normal eyelid closure. If it were the JNK phosphorylation level that determines eyelid closure outcome, we might expect that a reduction of both JNK1 and JNK2 would disturb normal eyelid development. To evaluate this possibility, we generated $Mekk1^{+/\Delta KD}Jnk1^{+/-}Jnk2^{+/-}$ triple hemizygous mice, in which the gene dosage for each of the three components was reduced to a half. Interestingly, the triple hemizygotes displayed partial embryonic eyelid closure, in contrast to the *Jnk1*/*Jnk2*, *Mekk1*/*Jnk1* and *Mekk1*/*Jnk2* double hemizygous fetuses, which had normal eyelid development and closure at E16.5 (Fig. 7A and data not shown). Examination of the triple hemizygous E15.5 fetuses showed much less JNK phosphorylation, and more importantly, a significantly reduced c-Jun phosphorylation in the developing eyelid epithelium (Fig. 7A), indicating that the downstream pathways affected in the triple hemizygous were similar to those in $Mekk1^{\Delta KD/\Delta KD}$ and $Mekk1^{+/\Delta KD}Jnk1^{-/-}$ fetuses. We therefore suggest that JNK1 and JNK2 cooperate in transmitting MEKK1 eyelid closure signals and that the MEKK1-JNK1/JNK2 axis coordinates in the extent of JNK activation to set off the downstream pathway activation (Fig. 7B).

## DISCUSSION

Our results show that JNK1 and JNK2 act in concert but show a large difference in their relative contributions to epithelial morphogenesis. Three lines of evidence support this conclusion: first, JNK1 and JNK2 are equally expressed, but are differentially phosphorylated in the eyelid epithelium; second, activin B and MEKK1 signals cause twice as much phosphorylation of JNK1 than of JNK2 in cultured cells; third, in the $Mekk1^{+/\Delta KD}$genetic background, $Jnk1^{-/-}$, but not $Jnk2^{-/-}$ mice, develop EOB, suggesting differential contributions of the JNK isoforms.

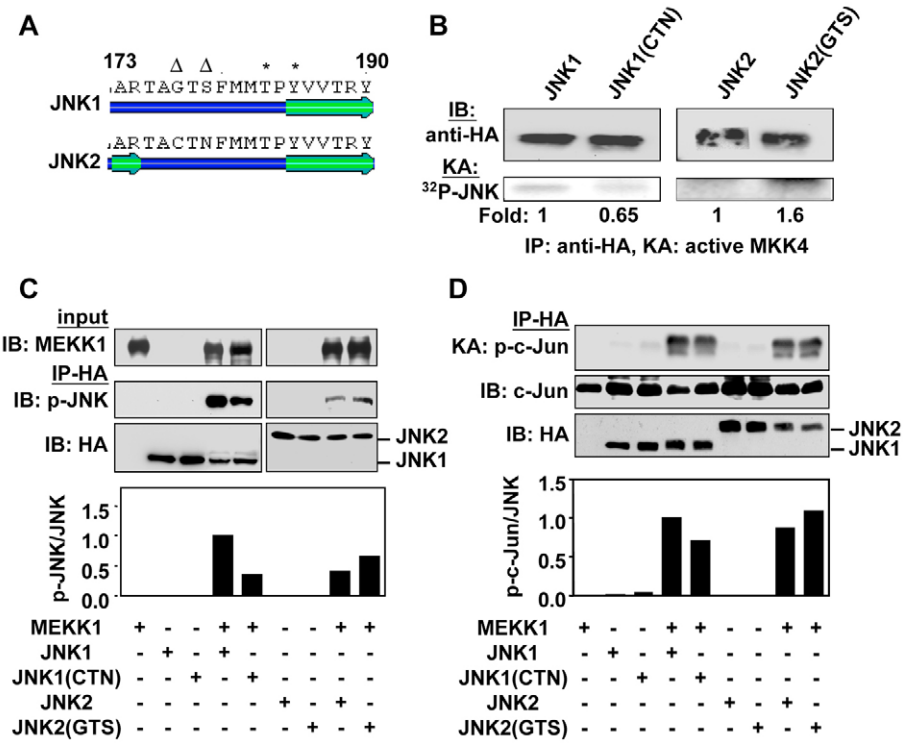


**Fig. 6. The G177/S179 residues in the JNK1 are crucial for its activity** (**A**) SABLE analysis revealed a putative structural difference between JNK1 and JNK2 in the variable region. The arrows represent β-strands that are predicted in this region. An extra β-strand is predicted in JNK2, but not in JNK1. Asterisks identify the Thr and Tyr residues as JNK phosphate acceptor sites. The triangles indicate the G177/S179 residues in JNK1, which are divergent from C177/N179 in JNK2. (**B**) HEK293 cells were transiently transfected with wild-type HA-JNK1 and HA-JNK2, and mutant HA-JNK1 (CTN) and HA-JNK2 (GTS). The JNK proteins were isolated by immunoprecipitation using HA-conjugated beads and subjected to western blotting using anti-HA followed by quantification using chemiluminescence imaging analyses. The precipitates were also used for an in vitro kinase assay with an active MKK4 as the kinase in the presence of [γ-$^{32}$P]ATP. JNK phosphorylation was detected by exposure to X-ray film and phosphoimager analyses. The values of the relative $^{32}$P-JNK/total JNK of the mutants were compared with that of their wild-type counterparts, which were designated as 1. (**C**,**D**) HEK293 cells were transiently co-transfected with active MEKK1, wild-type HA-JNK1 and HA-JNK2, and mutant HA-JNK1 (CTN) and HA-JNK2 (GTS), as indicated. The cell lysates were analyzed for MEKK1 expression by western blot analyses and were used for immunoprecipitation with anti-HA. The immunoprecipitates (C) were analyzed for the phospho- and total-JNK by western blotting and chemiluminescence imaging analyses, and (D) were subjected to in vitro kinase assay (KA) using GST-c-Jun as a substrate in the presence of [γ-$^{32}$P]ATP. The GST-c-Jun phosphorylation was detected by exposure to X-ray film and the GST-c-Jun and JNK proteins in the reaction were detected by western blot. The relative p-c-Jun/total c-Jun levels were calculated and are shown in the graph. Consistent results were obtained from at least three independent experiments.

Possible mechanisms underlying functional differences of JNK isoforms include selective localization, distinct interactions with upstream regulators and downstream substrates, and different substrate preferences (Bogoyevitch and Kobe, 2006); however, none of these seem to adequately explain the differential JNK isoform phosphorylation observed in developing eyelid epithelium (Fig. 5B and see Fig. S3B,C in the supplementary material). We find subtle structural differences between JNK1 and JNK2 in a variable region (amino acids 173-190) that encompasses the phosphate-acceptor sites at Thr183 and Tyr185 (Xie et al., 1998). Specifically, although JNK1 appears to have a propensity for a less-ordered structure within the variable region that may favor efficient phosphorylation, JNK2 adopts a more rigid β-strand conformation within the activation loop, which may reduce its accessibility to the upstream MKK4. The Gly177 and Ser179 residues of JNK1 are largely responsible for its efficient phosphorylation, and their replacement with the corresponding Cys177 and Asn179 residues of JNK2 causes a significant reduction of phosphorylation by MKK4 and MEKK1 signals. The intrinsic differences between JNK1 and JNK2 in phosphorylation efficiency explain very well the unique roles displayed by the JNK isoforms in transmitting MEKK1-mediated morphogenic signals.

It is interesting to find that the *Mekk1*$^{+/\Delta KD}$*Jnk1*$^{+/-}$*Jnk2*$^{+/-}$ compound mutant mice have partial EOB, underlining that, apart from their differences, the JNK isoforms also have complementary functions in transmitting MEKK1 signals. Similar functional interactions between JNK1 and JNK2 have previously been observed in compound JNK mutant mice, revealing a predominant role of JNK1 in glucose metabolism and optic fissure and eyelid closure, which can be at least partly compensated by JNK2 (Tuncman et al., 2006; Weston et al., 2003). Thus, the differential and complementary roles of JNK1 and JNK2 may well be an underlying mechanism through which the JNK isoforms operate in many other in vivo processes.

From an evolutionary standpoint, mammalian *Jnk1* and *Jnk2* genes are probably derived from a gene duplication event, because JNK1 has preserved the Gly177 and Ser179 residues also present in *Drosophila* JNK, whereas JNK2 has diverged from the common ancestor on these residues. Such subtle diversification may allow the JNK isoforms to have slightly divergent, but at the same time similar functions, which perhaps is just what the organism needs for preserving redundancy of this important protein kinase, but at the same time, offering variations in their regulation and function. On one hand, JNK1 may be more important than JNK2 in preserving the ancestral functions in epithelial morphogenesis. On the other hand, JNK1 and JNK2 closely resemble each other, sharing many common features and exhibiting functional similarities. The redundancy of the JNK isoforms may serve as a protection measure of higher eukaryotes from defects caused by a single *Jnk* gene mutation, such as those seen in *Drosophila* (Agnes et al., 1999; Kuan et al., 1999; Sabapathy et al., 2001).

It is worth noting that distinct and even opposite roles of the JNK isoforms have been reported in T-cell differentiation, neuronal function, inflammation and tumorigenesis (Chang et al., 2003; Chen et al., 2001; Han et al., 2002; Sabapathy et al., 2001). Hence, cooperative interplay of JNK1 and JNK2 appears to be tissue- and

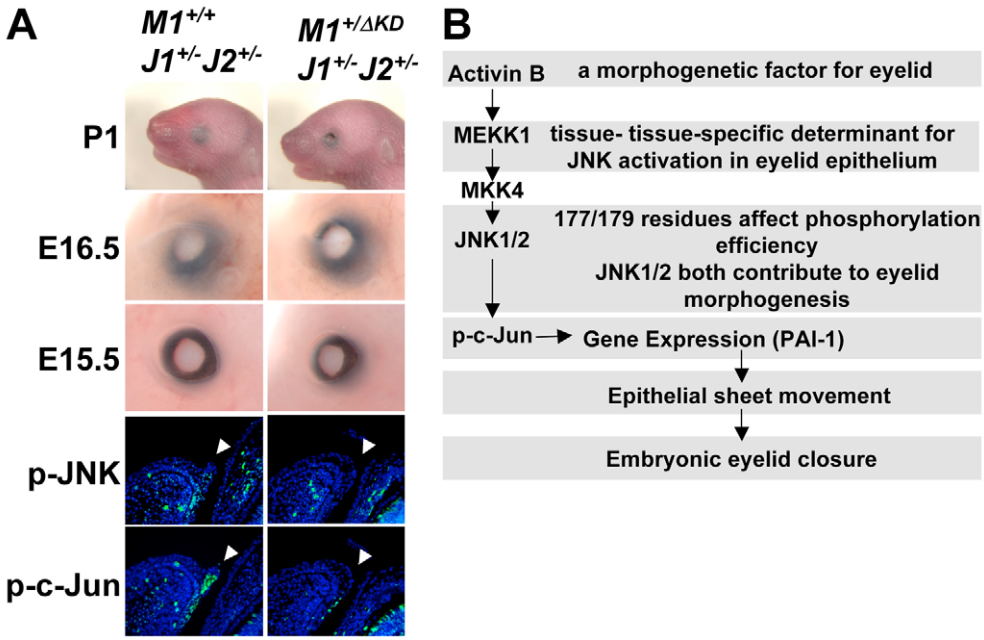


**Fig. 7. *Mekk1*, *Jnk1* and *Jnk2* gene doses are crucial for embryonic eyelid closure.** (**A**) $M1^{+/\Delta KD}J1^{+/-}J2^{+/-}$ triple heterozygous mice have EOB phenotype at postnatal day 1, with a partially exposed ocular surface at E16.5; by contrast, the $M1^{+/+}J1^{+/-}J2^{+/-}$ mice had closed eyelids at E16.5 and P1. The developing eye at E15.5 shows less phosphorylation of JNK and c-Jun (green) in the eyelid epithelium (arrowheads) of the triple hemizygous compared with the double hemizygous fetuses. (**B**) Diagram illustrating the signaling pathways in the control of eyelid epithelial morphogenesis. The signal is initiated from the eyelid morphogenetic factor activin B, which leads to the activation of MEKK1, a tissue-specific and rate-limiting determinant for transmitting the activin B signals. MEKK1 activates MKK4, which in turn phosphorylates JNK1 and JNK2. Because of the intrinsic variable sequence difference between the JNK isoforms, JNK1 is more effectively phosphorylated than JNK2. The total phospho-JNK determines the nuclear transcription factor c-Jun phosphorylation and induction of gene expression, such as PAI1. The endpoint of this pathway activation is the induction of epithelial cell migration, and eyelid epithelial morphogenesis and closure.

function-specific and may be largely determined by the upstream regulatory signaling pathways. In the developing eyelid epithelium, JNK activity is specifically regulated by activin B signals transmitted by MEKK1 mainly through MKK4 (Cuenda and Dorow, 1998; Xia et al., 1998). Although MEKK1 acts as a tissue-specific and rate-limiting factor for JNK activation, the levels of JNK activity determine downstream c-Jun phosphorylation and PAI1 expression, and consequently, epithelial cell migration and eyelid closure (Fig. 7B). In light of these findings, we suggest that the MAP3Ks are key regulatory molecules for determining the activities and functions of JNK1 and JNK2 in a signal- and tissue-specific manner.

We thank Alvaro Puga, Winston Kao, Xinhua Lin, Peter Stambrook and Yi Zheng for a critical reading of the manuscript, Michael Karin for providing *Jnk1*$^{-/-}$ and *Jnk2*$^{-/-}$ mice, Hiroshi Nishina for providing MKK4-deficient cells, Maureen Mongan for help with maintaining mouse colonies and genotyping and Maureen Sartor for helpful discussions on gene-dose effect. This work is supported in part by NIH grants EY15227 (Y.X.). E.G. is a Predoctoral Trainee supported by NIEHS T32 ES07250, Environmental Carcinogenesis and Mutagenesis Training Grant.

**Supplementary material**

Supplementary material for this article is available at
http://dev.biologists.org/cgi/content/full/135/1/23/DC1

**References**

**Adamczak, R., Porollo, A. and Meller, J.** (2004). Accurate prediction of solvent accessibility using neural networks-based regression. *Proteins* **56**, 753-767.

**Agnes, F., Suzanne, M. and Noselli, S.** (1999). The Drosophila JNK pathway controls the morphogenesis of imaginal discs during metamorphosis. *Development* **126**, 5453-5462.

**Bocco, J. L., Bahr, A., Goetz, J., Hauss, C., Kallunki, T., Kedinger, C. and Chatton, B.** (1996). In vivo association of ATFa with JNK/SAP kinase activities. *Oncogene* **12**, 1971-1980.

**Bogoyevitch, M. A. and Kobe, B.** (2006). Uses for JNK: the many and varied substrates of the c-Jun N-terminal kinases. *Microbiol. Mol. Biol. Rev.* **70**, 1061-1095.

**Chang, L., Jones, Y., Ellisman, M. H., Goldstein, L. S. and Karin, M.** (2003). JNK1 is required for maintenance of neuronal microtubules and controls phosphorylation of microtubule-associated proteins. *Dev. Cell* **4**, 521-533.

**Chen, N., Nomura, M., She, Q. B., Ma, W. Y., Bode, A. M., Wang, L., Flavell, R. A. and Dong, Z.** (2001). Suppression of skin tumorigenesis in c-Jun NH (2)-terminal kinase-2-deficient mice. *Cancer Res.* **61**, 3908-3912.

**Cuenda, A. and Dorow, D. S.** (1998). Differential activation of stress-activated protein kinase kinases SKK4/MKK7 and SKK1/MKK4 by the mixed-lineage kinase-2 and mitogen-activated protein kinase kinase (MKK) kinase-1. *Biochem. J.* **333**, 11-15.

**Davis, R. J.** (2000). Signal transduction by the JNK group of MAP kinases. *Cell* **103**, 239-252.

**Deng, M., Chen, W. L., Takatori, A., Peng, Z., Zhang, L., Mongan, M., Parthasarathy, R., Sartor, M., Miller, M., Yang, J. et al.** (2006). A role for the mitogen-activated protein kinase kinase kinase 1 in epithelial wound healing. *Mol. Biol. Cell* **17**, 3446-3455.

**Derijard, B., Hibi, M., Wu, I. H., Barrett, T., Su, B., Deng, T., Karin, M. and Davis, R. J.** (1994). JNK1: a protein kinase stimulated by UV light and Ha-Ras that binds and phosphorylates the c-Jun activation domain. *Cell* **76**, 1025-1037.

**Dong, C., Yang, D. D., Wysk, M., Whitmarsh, A. J., Davis, R. J. and Flavell, R. A.** (1998). Defective T cell differentiation in the absence of Jnk1. *Science* **282**, 2092-2095.

**Eminel, S., Klettner, A., Roemer, L., Herdegen, T. and Waetzig, V.** (2004). JNK2 translocates to the mitochondria and mediates cytochrome c release in PC12 cells in response to 6-hydroxydopamine 1. *J. Biol. Chem.* **279**, 55385-55392.

**Gao, M., Labuda, T., Xia, Y., Gallagher, E., Fang, D., Liu, Y. C. and Karin, M.** (2004). Jun turnover is controlled through JNK-dependent phosphorylation of the E3 ligase Itch. *Science* **306**, 271-275.

**Gdalyahu, A., Ghosh, I., Levy, T., Sapir, T., Sapoznik, S., Fishler, Y., Azoulai, D. and Reiner, O.** (2004). DCX, a new mediator of the JNK pathway. *EMBO J.* **23**, 823-832.

**Giroux, S., Tremblay, M., Bernard, D., Cardin-Girard, J. F., Aubry, S., Larouche, L., Rousseau, S., Huot, J., Landry, J., Jeannotte, L. et al.** (1999). Embryonic death of Mek1-deficient mice reveals a role for this kinase in angiogenesis in the labyrinthine region of the placenta. *Curr. Biol.* **9**, 369-372.
**Han, Z., Chang, L., Yamanishi, Y., Karin, M. and Firestein, G. S.** (2002). Joint damage and inflammation in c-Jun N-terminal kinase 2 knockout mice with passive murine collagen-induced arthritis. *Arthritis Rheum.* **46**, 818-823.
**Kuan, C. Y., Yang, D. D., Samanta Roy, D. R., Davis, R. J., Rakic, P. and Flavell, R. A.** (1999). The Jnk1 and Jnk2 protein kinases are required for regional specific apoptosis during early brain development. *Neuron* **22**, 667-676.
**Kyriakis, J. M., Woodgett, J. R. and Avruch, J.** (1995). The stress-activated protein kinases. A novel ERK subfamily responsive to cellular stress and inflammatory cytokines. *Ann. N. Y. Acad. Sci.* **766**, 303-319.
**Li, G., Gustafson-Brown, C., Hanks, S. K., Nason, K., Arbeit, J. M., Pogliano, K., Wisdom, R. M. and Johnson, R. S.** (2003). c-Jun is essential for organization of the epidermal leading edge. *Dev. Cell* **4**, 865-877.
**Liu, J., Minemoto, Y. and Lin, A.** (2004). c-Jun N-terminal protein kinase 1 (JNK1), but not JNK2, is essential for tumor necrosis factor alpha-induced c-Jun kinase activation and apoptosis. *Mol. Cell. Biol.* **24**, 10844-10856.
**Nishina, H., Vaz, C., Billia, P., Nghiem, M., Sasaki, T., De la Pompa, J. L., Furlonger, K., Paige, C., Hui, C., Fischer, K. D. et al.** (1999). Defective liver formation and liver cell apoptosis in mice lacking the stress signaling kinase SEK1/MKK4. *Development* **126**, 505-516.
**Noselli, S. and Agnes, F.** (1999). Roles of the JNK signaling pathway in Drosophila morphogenesis. *Curr. Opin. Genet. Dev.* **9**, 466-472.
**Sabapathy, K., Hu, Y., Kallunki, T., Schreiber, M., David, J. P., Jochum, W., Wagner, E. F. and Karin, M.** (1999). JNK2 is required for efficient T-cell activation and apoptosis but not for normal lymphocyte development. *Curr. Biol.* **9**, 116-125.
**Sabapathy, K., Kallunki, T., David, J. P., Graef, I., Karin, M. and Wagner, E. F.** (2001). c-Jun NH2-terminal kinase (JNK)1 and JNK2 have similar and stage-dependent roles in regulating T cell apoptosis and proliferation. *J. Exp. Med.* **193**, 317-328.
**Schlesinger, T. K., Fanger, G. R., Yujiri, T. and Johnson, G. L.** (1998). The TAO of MEKK. *Front. Biosci.* **3**, 1181-1186.
**Sluss, H. K., Han, Z., Barrett, T., Davis, R. J. and Ip, Y. T.** (1996). A JNK signal transduction pathway that mediates morphogenesis and an immune response in Drosophila. *Genes Dev.* **10**, 2745-2758.
**Tuncman, G., Hirosumi, J., Solinas, G., Chang, L., Karin, M. and Hotamisligil, G. S.** (2006). Functional in vivo interactions between JNK1 and JNK2 isoforms in obesity and insulin resistance. *Proc. Natl. Acad. Sci. USA* **103**, 10741-10746.
**Vassalli, A., Matzuk, M. M., Gardner, H. A., Lee, K. F. and Jaenisch, R.** (1994). Activin/inhibin beta B subunit gene disruption leads to defects in eyelid development and female reproduction. *Genes Dev.* **8**, 414-427.
**Ventura, J. J., Hubner, A., Zhang, C., Flavell, R. A., Shokat, K. M. and Davis, R. J.** (2006). Chemical genetic analysis of the time course of signal transduction by JNK. *Mol. Cell* **21**, 701-710.
**Weston, C. R., Wong, A., Hall, J. P., Goad, M. E., Flavell, R. A. and Davis, R. J.** (2003). JNK initiates a cytokine cascade that causes Pax2 expression and closure of the optic fissure. *Genes Dev.* **17**, 1271-1280.
**Xia, Y. and Karin, M.** (2004). The control of cell motility and epithelial morphogenesis by Jun kinases. *Trends Cell Biol.* **14**, 94-101.
**Xia, Y., Wu, Z., Su, B., Murray, B. and Karin, M.** (1998). JNKK1 organizes a MAP kinase module through specific and sequential interactions with upstream and downstream components mediated by its amino-terminal extension. *Genes Dev.* **12**, 3369-3381.
**Xie, X., Gu, Y., Fox, T., Coll, J. T., Fleming, M. A., Markland, W., Caron, P. R., Wilson, K. P. and Su, M. S.** (1998). Crystal structure of JNK3: a kinase implicated in neuronal apoptosis. *Structure* **6**, 983-991.
**Xu, S. and Cobb, M. H.** (1997). MEKK1 binds directly to the c-Jun N-terminal kinases/stress-activated protein kinases. *J. Biol. Chem.* **272**, 32056-32060.
**Zhang, L., Wang, W., Hayashi, Y., Jester, J. V., Birk, D. E., Gao, M., Liu, C. Y., Kao, W. W., Karin, M. and Xia, Y.** (2003). A role for MEK kinase 1 in TGF-beta/activin-induced epithelium movement and embryonic eyelid closure. *EMBO J.* **22**, 4443-4454.
**Zhang, L., Deng, M., Parthasarathy, R., Wang, L., Mongan, M., Molkentin, J. D., Zheng, Y. and Xia, Y.** (2005). MEKK1 transduces activin signals in keratinocytes to induce actin stress fiber formation and migration. *Mol. Cell. Biol.* **25**, 60-65.